Dynamic Modeling and Stability Analysis of Onboard DC Power System for Hybrid Electric Ships

Daeseong Park
Department of Marine Technology
Norwegian University of Science and Technology
Trondheim, Norway
Email: daeseong.park@ntnu.no

Mehdi Karbalaye Zadeh
Department of Marine Technology
Norwegian University of Science and Technology
Trondheim, Norway
Email: mehdi.zadeh@ntnu.no

***Abstract*—This paper presents the dynamic modeling and stability analysis of the onboard DC power system, applicable to hybrid electric ships. The system topology is established with a special focus on the integration of the energy carriers with power electronic converters. The modeling of the AC/DC rectifier, DC/DC converter, filters and energy storage systems (ESS), such as battery and supercapacitor, is investigated. AC/DC rectifier is modeled with decoupling control through an LCL filter, and the DC/DC converter modeling is compared with the state-space averaging method and generalized averaging method. The performance of the integrated model is presented both in charging mode and in discharging mode of the energy storage system and the results show the effectiveness of the controllers and the power regulation of the ESSs. In the end, the limitation of the load is obtained by the stability analysis.**

***Index Terms*—Hybrid power systems, Onboard DC power systems, Electrification, Hybrid ships, Stability, Dynamic modeling**

I. Introduction

Consequently to the recent developments in the technology of power electronics, onboard DC power systems have received a great interest and have been widely used for transportation electrification such as electric vehicles, more electric aircrafts and electrified ships [1], [2], [3]. Shipboard DC power systems have been recently proposed as an alternative propulsion system in the marine industry because of the natural flexibility and improved operability of DC power system compared to the conventional AC system, which allows the DC connected generators to be operated with their optimal speed at the required load level and brings significant economical and environmental values for the shipping industry [4]. The optimal operation of the shipboard generators reduces the fuel oil consumption of the ship that leads to lower operating cost and emissions. In addition, the DC power system can easily integrate energy storage systems (ESSs) such as batteries, supercapacitors and fuel cells, and they enable even cleaner and optimized sailing of the ship. With the recent technological developments, DC power systems have been even more applicable and they have been installed for the small ferries. However, instability is still a major issue in the design of DC power systems necessitating reliable modeling tools [5] and particularly with multiple converter-controlled propulsion drives acting as constant power load (CPL) [6]. Catching up with this trend, an overview of the modeling and control for the shipboard DC power systems have been studied. The main objective of this paper is to investigate mathematical modeling methodologies with an emphasis on the power electronics so that they can be used for stability analysis and control. In the end, all the components are integrated and simulated at the same time to observe the performance of the modeling and controllers. The outline of this paper consists of each component modeling in the onboard DC power systems, control method for the power electronics, the simulation results and the stability analysis.

II. Modeling of Onboard DC Power System

A. Design of the onboard DC power system

In Figure 1, the electric circuit of onboard DC power system for this paper is presented. The system is simplified, but it is modeled to include all the components that comprise the onboard DC power system with AC sources, LCL filter, AC/DC rectifier, DC/DC converters, energy storage systems and power loads.

B. AC source and AC/DC converter

Instead of building a synchronous generator with a diesel engine, pure AC voltage sources for each phase are used as sine waves for the simplification. A similar modeling approach is used and detailed in [7]. Then, the voltage and current equations from the LCL filter (without passive damping) are modeled for phase A as shown in (1)-(4), which will be transformed to dq-frame in (5)-(6) for the control purpose. For the other phases, the equations are the same with different subscripts. In the modeling, D_i represents $D_{upper} - D_{lower}$ as a control signal of IGBTs operations as each D signal have a value of 1 (close) or 0 (open), and D_{ESS} means charging or discharging mode of the energy storage systems.

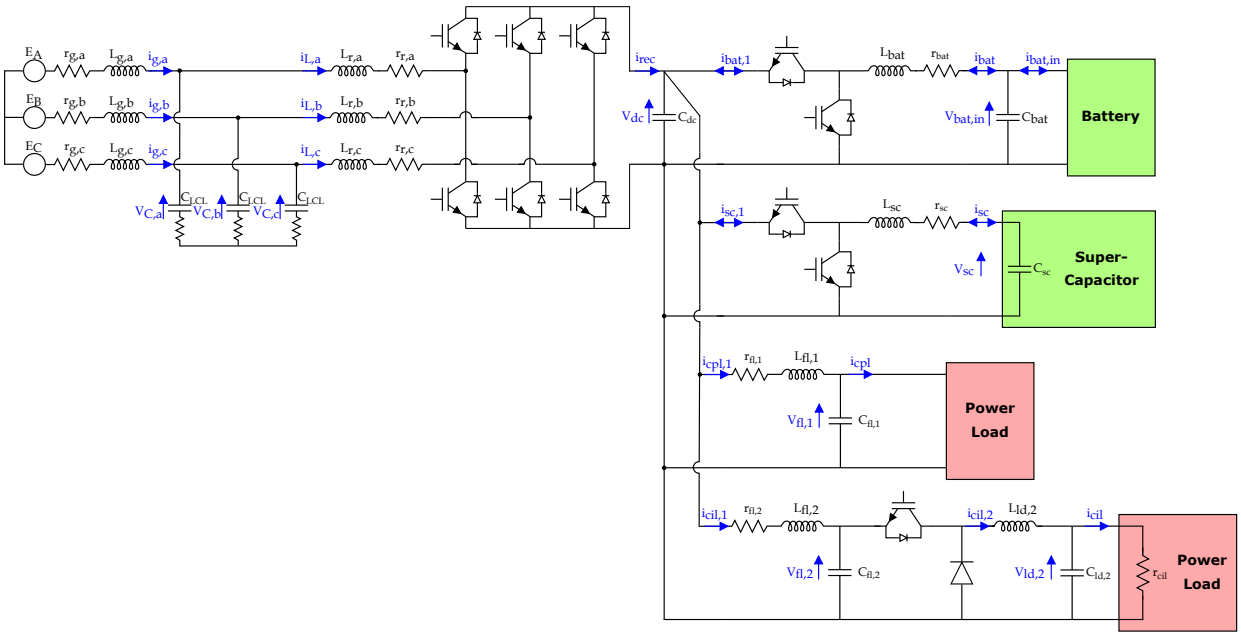

Fig. 1. Electric Circuit Diagram of the Proposed Onboard DC Power System under Investigation

$$L_{g,a}\frac{di_{g,a}}{dt} = E_A - i_{g,a}r_{g,a} - v_{C,a} \tag{1}$$

$$C_{LCL}\frac{dv_{C,a}}{dt} = i_{g,a} - i_{L,a} \tag{2}$$

$$L_{r,a}\frac{i_{L,a}}{dt} = v_{C,a} - i_{L,a}r_{r,a} - D_1V_{dc} \tag{3}$$

$$C_{dc}\frac{dV_{dc}}{dt} = D_1i_{L,a} + D_2i_{L,b} + D_3i_{L,c} - \sum_j i_{load,j} + \sum_k D_{ESS,k}i_{ESS,k} \tag{4}$$

$$L_{g,a}\frac{di_d}{dt} = E_d - i_dr_d - v_{C,d} + L_{g,a}\omega i_q \tag{5}$$

$$L_{g,a}\frac{di_q}{dt} = E_q - i_qr_q - v_{C,q} - L_{g,a}\omega i_d \tag{6}$$

C. DC/DC converter

For DC/DC converters, averaging methods are considered with state-space averaging and generalized averaging as explained in [8], [9]. First, DC/DC converter equations in state-space form can be obtained from the circuit as (7) for boost mode and (8) for buck mode. To derive equations of DC/DC converters, a virtual resistor element of R and a subscript 1 for higher voltage side or 2 for lower voltage side are used for the simplified derivation.

$$\frac{d\bar{\mathbf{x}}(t)}{dt} = \frac{d}{dt}\begin{bmatrix}\overline{i_L}\\ \overline{v_C}\end{bmatrix} = \left((1-d)\begin{bmatrix}0 & -\frac{1}{nL}\\ \frac{1}{nC} & -\frac{1}{CR}\end{bmatrix} + d\begin{bmatrix}0 & 0\\ 0 & -\frac{1}{CR}\end{bmatrix}\right)\bar{\mathbf{x}}(t) + \begin{bmatrix}\frac{1}{nL}\\ 0\end{bmatrix}\overline{v_{in}}(t) \tag{7}$$

$$\frac{d\bar{\mathbf{x}}(t)}{dt} = \begin{bmatrix}0 & -\frac{1}{L}\\ \frac{1}{C} & -\frac{1}{CR}\end{bmatrix}\bar{\mathbf{x}}(t) + d\begin{bmatrix}\frac{1}{nL}\\ 0\end{bmatrix}\overline{v_{in}}(t) \tag{8}$$

The generalized averaging method was introduced by [11] in 1991, and [8] studied for modeling and simulation of multi-converter DC power electronic systems by using this method. While the state-space averaging method is susceptible to large-signal variations and oscillating behaviour for the state variables, the generalized averaging method enables to model various kinds of converters with large-signal and different waveforms of state variables. Hereafter, the derivation of the model for the buck-boost converter by using the generalized averaging method is briefly explained. First, this method utilizes the fact that the time-domain waveform $x(\tau)$ can be approximated by Fourier series:

$$x(\tau) = \sum_{k=-\infty}^{\infty} X_k(t)e^{jk\omega_s\tau}, \text{ for } \tau \in (t-T, t] \tag{9}$$

where, $\omega_s = \frac{2\pi}{T}$, T is approximated time interval and $X_k(t)$ is the complex Fourier coefficients. Also, the kth coefficient at time t is determined by the following averaging operation and $\langle x\rangle_k(t)$ is denoted as an averaging operation.

$$X_k(t) = \frac{1}{T}\int_{t-T}^{t} x(\tau)e^{-jk\omega_s\tau}d\tau = \langle x\rangle_k(t) \tag{10}$$

By using these operations, the aim is to derive a state-space model having $\langle x\rangle_k$ as state variables. For buck mode of operation, the commutation function $u(t)$ can be defined as:

$$u(t) = \begin{cases} 1, & 0 < t < dT \\ 0, & dT < t < T \end{cases} \tag{11}$$

where, d is duty cycle, T is switching period. Then, the Fourier

coefficients of the states such as i_L and v_C can be estimated by using the first-order approximation as:

$$\langle i_L \rangle_1 = x_1 + jx_2, \langle i_L \rangle_0 = x_5 \tag{12a}$$
$$\langle v_o \rangle_1 = x_3 + jx_4, \langle v_o \rangle_0 = x_6 \tag{12b}$$
$$\langle i_L \rangle_{-1} = \langle i_L \rangle_1^*, \langle v_o \rangle_{-1} = \langle v_o \rangle_1^* \tag{12c}$$

where the operator * denotes the conjugate of a complex number. Since i_L and v_C are real, (12c) can be derived. Then, by using (10), i_L and v_C are derived by using six states of the generalized averaging method as:

$$i_L = x_5 + 2x_1 cos\omega t - 2x_2 sin\omega t \tag{13a}$$
$$v_o = x_6 + 2x_3 cos\omega t - 2x_4 sin\omega t \tag{13b}$$

Now, it is possible to derive the differential equations for x_1, x_2, x_3, x_4, x_5 and x_6 by using the method of undetermined coefficients, and they are expressed in state-space form of the buck mode as:

$$\begin{bmatrix} \dot{x}_1 \\ \dot{x}_2 \\ \dot{x}_3 \\ \dot{x}_4 \\ \dot{x}_5 \\ \dot{x}_6 \end{bmatrix} = \begin{bmatrix} 0 & \omega & -\frac{1}{L} & 0 & 0 \\ 0 & & & & \\ -\omega & 0 & 0 & -\frac{1}{L} & 0 \\ 0 & & & & \\ \frac{1}{C_1} & 0 & -\frac{1}{R_1 C_1} & \omega & 0 \\ 0 & & & & \\ 0 & \frac{1}{C_1} & -\omega & -\frac{1}{R_1 C_1} & 0 \\ 0 & & & & \\ 0 & 0 & 0 & 0 & 0 \\ -\frac{1}{L} & & & & \\ 0 & 0 & 0 & 0 & \frac{1}{C_1} \\ -\frac{1}{R_1 C_1} & & & & \end{bmatrix} \begin{bmatrix} x_1 \\ x_2 \\ x_3 \\ x_4 \\ x_5 \\ x_6 \end{bmatrix} + \begin{bmatrix} \frac{d}{nL} & 0 & \frac{sin(2\pi d)}{2n\pi L} \\ 0 & \frac{d}{nL} & -\frac{1-cos(2\pi d)}{2n\pi L} \\ -\frac{1-cos(\pi d)}{2n\pi L} & -\frac{1-cos(\pi d)}{2n\pi L} & -\frac{1-cos(\pi d)}{2n\pi L} \\ 0 & 0 & 0 \\ \frac{sin(2\pi d)}{n\pi L} & -\frac{1-cos(2\pi d)}{n\pi L} & \frac{d}{nL} \\ -\frac{1-cos(\pi d)}{2n\pi L} & -\frac{1-cos(\pi d)}{2n\pi L} & -\frac{1-cos(\pi d)}{2n\pi L} \end{bmatrix} \begin{bmatrix} Re\langle v_{in} \rangle_1 \\ Im\langle v_{in} \rangle_1 \\ \langle v_{in} \rangle_0 \end{bmatrix} \tag{14}$$

Similarly, the state-space form of the boost mode based on the generalized averaging method can be derived as:

$$\begin{bmatrix} \dot{x}_1 \\ \dot{x}_2 \\ \dot{x}_3 \\ \dot{x}_4 \\ \dot{x}_5 \\ \dot{x}_6 \end{bmatrix} = \begin{bmatrix} 0 & \omega & -\frac{1-d}{nL} & 0 & 0 \\ \frac{sin(2\pi d)}{2n\pi L} & & & & \\ -\omega & 0 & 0 & -\frac{1-d}{nL} & 0 \\ -\frac{1-cos(2\pi d)}{2n\pi L} & & & & \\ \frac{1-d}{nC_2} & 0 & -\frac{1}{R_2 C_2} & \omega & -\frac{sin(2\pi d)}{2n\pi C_2} \\ 0 & & & & \\ 0 & \frac{1-d}{nC_2} & -\omega & -\frac{1}{R_2 C_2} & \frac{1-cos(2\pi d)}{2n\pi C_2} \\ 0 & & & & \\ 0 & 0 & \frac{sin(2\pi d)}{n\pi L} & -\frac{1-cos(2\pi d)}{n\pi L} & 0 \\ -\frac{1-d}{nL} & & & & \\ -\frac{sin(2\pi d)}{n\pi C_2} & \frac{1-cos(2\pi d)}{n\pi C_2} & 0 & 0 & \frac{1-d}{nC_2} \\ -\frac{1}{R_2 C_2} & & & & \end{bmatrix} \begin{bmatrix} x_1 \\ x_2 \\ x_3 \\ x_4 \\ x_5 \\ x_6 \end{bmatrix} + \begin{bmatrix} \frac{1}{L} & 0 & 0 \\ 0 & \frac{1}{L} & 0 \\ 0 & 0 & 0 \\ 0 & 0 & 0 \\ 0 & 0 & \frac{1}{L} \\ 0 & 0 & 0 \end{bmatrix} \begin{bmatrix} Re\langle v_{in} \rangle_1 \\ Im\langle v_{in} \rangle_1 \\ \langle v_{in} \rangle_0 \end{bmatrix} \tag{15}$$

Then, the converter model in boost mode is simulated as seen in Figure 2 for the cases of $n = 1, 2, 3$ (turn ratio for isolation) with the parameters listed in Table I.

TABLE I
CONVERTER PARAMETERS

Parameter	Value
Capacitance	5 mF
Inductance	516 mH
n (turns ratio)	3
$f_{sw,conv}$	2000 Hz

In Figure 2, the ripple in the generalized averaging method is clearly seen, and the results of the state-space averaging method show the averaged value of the generalized averaging method. In this regard, the state-space averaging method can be considered as a filtered or averaged method of the generalized averaging method. Therefore, the state-space averaging can be used as a low-pass filter or an observer model. In boost mode, the duty cycle is fixed at $d = 0.5$ as well, but in case of $n = 2$ or $n = 3$, the output voltage exceeds the DC voltage. In this mode, the battery output voltage is assumed to be $400V$, but the result shows that it can be difficult to control the output voltage to be in accordance with the DC voltage without a controller. In addition, a higher turn ratio should be avoided for the coordination of the voltage level between the grid and the battery.

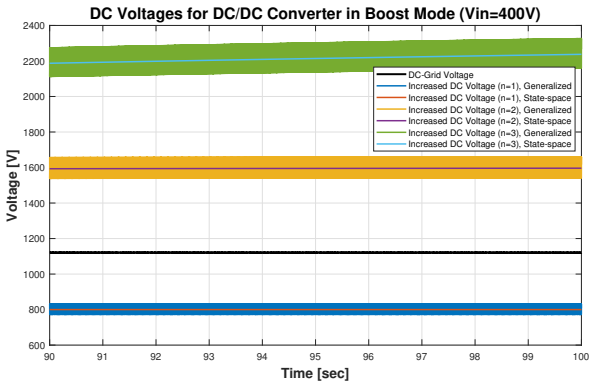

Fig. 2. Simulation of DC/DC Converter in Boost Mode

D. Battery (electrochemical) and supercapacitor

Battery model including internal resistance, terminal voltage, open circuit voltage, discharge current and the state of charge is developed by [12] and [13] modified this model to be compatible with Li-ion battery by considering a polarisation voltage instead of a polarisation resistance. The mathematical equations are be given with the parameters in Table II as:

$$V_{batt} = E_0 - R \cdot i - K\left(\frac{Q}{Q - \int_0^t idt}\right) \cdot \left(\int_0^t idt + i^*\right) + Ae^{-B \times \int_0^t idt} \tag{16}$$

$$V_{batt} = E_0 - R \cdot i - K\left(\frac{Q}{\int_0^t idt - 0.1Q}\right) i^* - K\left(\frac{Q}{Q - \int_0^t idt}\right) \cdot \int_0^t idt + Ae^{-B \times \int_0^t idt} \tag{17}$$

where,

V_{batt}= battery voltage (V)
E_0= battery constant voltage (V)
K= polarisation constant (V/Ah) or resistance (Ω)
Q= battery capacity (Ah)
$\int idt$= actual battery charge (Ah)
A= exponential zone amplitude (V)
B= exponential zone time constant inverse $(\text{Ah})^{-1}$
R= internal resistance (R)
i= battery current (A)
i^*= filtered battery current (A)

The supercapacitor is modeled as a simple capacitor without the consideration of the frequency of the input voltage and current, temperature and voltage level. However, the operating range of the energy of the supercapacitor is limited with the minimum and maximum voltage. Then, the energy of the supercapacitor E_{sc} is controlled by $\Delta E_{sc} = \frac{1}{2}C_{sc}(V_{sc,max}^2 - V_{sc,min}^2)$.

TABLE II
BATTERY MODEL PARAMETERS

Parameter	Value
E_0	850 V
Q	1200 Ah
K	0.0006 Ω
A	0.9 V
B	100 Ah^{-1}
R	0.01 Ω

E. Loads

The constant power load that represents propulsion motors is fed through an LC filter to reduce the total distortion harmonics. The model equations become as (18)-(19). In this study, a resistive load that represents hotel load in the ship is also considered as a constant impedance load that is integrated through a buck DC/DC converter. The model equations become as (20)-(23).

$$L_{fl,1}\frac{di_{cpl,1}}{dt} = V_{dc} - i_{cpl,1}r_{fl,1} - V_{fl,1} \quad (18)$$

$$C_{fl,1}\frac{dV_{fl,1}}{dt} = i_{cpl,1} - i_{cpl} = i_{cpl,1} - \frac{P_{CPL}}{V_{fl,1}} \quad (19)$$

$$L_{fl,2}\frac{di_{cil,1}}{dt} = V_{dc} - i_{cil,1}r_{fl,2} - V_{fl,2} \quad (20)$$

$$C_{fl,2}\frac{dV_{fl,2}}{dt} = i_{cil,1} - i_{cil,2} \quad (21)$$

$$L_{ld,2}\frac{di_{cil,2}}{dt} = dV_{fl,2} - V_{ld,2} \quad (22)$$

$$C_{ld,2}\frac{dV_{ld,2}}{dt} = i_{cil,2} - i_{cil} = i_{cil,2} - \sqrt{\frac{P_{CIL}}{r_{cil}}} \quad (23)$$

III. CONTROL OF ONBOARD DC POWER SYSTEM

A. DC voltage control

The DC bus voltage is controlled by the rectifier. For the control of the output DC voltage from rectifier, decoupling control method is applied in the DQ synchronous reference frame where the three-phase voltage is transformed to DQ voltage by Park's transform. The DC voltage control approach is explained in [15]. The block diagram for the control is presented in Figure 3.

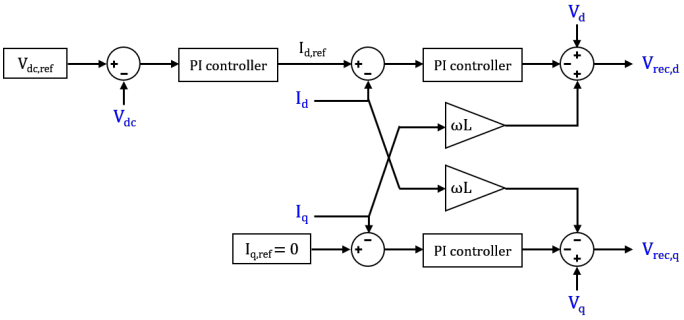

Fig. 3. Block Diagram for Control of V_{DC} and Reactive Current by DQ-Decoupling Control

B. Control of DC/DC converter

To control the output current of the DC/DC converter in buck mode, the sliding mode control is applied [16], and PI controller is applied for the boost mode. The sliding mode control starts with a function S with the current error and the integral term given in (where $\dot{S} = -\lambda S$) :

$$S = i_{L,mes} - i_{ref} + K_x \cdot \int_0^t (i_{L,mes} - i_{ref})d\tau \quad (24)$$

To calculate i_{ref}, the electric charge q $(= C_{DC}V_{DC})$ and its reference q_{ref} $(= C_{DC}V_{DC,ref})$ of the DC-link capacitor, the rate of the charge can be given as:

$$\dot{q} = \dot{q}_{ref} - \underbrace{K_{1v}}_{2\zeta\omega_n}(q - q_{ref}) - \underbrace{K_{2v}}_{\omega_n^2} \cdot \int_0^t (q - q_{ref})d\tau \quad (25)$$

Then, i_{ref} is defined as a sum of the measured current and the controlled rate of the electric charge. Then, the control scheme can be made for the buck mode of the DC/DC converter. The duty cycle of the DC/DC converter is calculated by using its mathematical equations as in (26).

$$D_{buck} = \frac{n}{V_{in}}\Big(V_{s,mes} + L \cdot (\dot{i_{ref}} - (i_{L,mes} - i_{ref})(K_x + \lambda) - \lambda K_x \cdot \int_0^t (i_{L,mes} - i_{ref})d\tau)\Big) \int_0^t (q - q_{ref})d\tau \quad (26)$$

IV. Simulation Results

With the mathematical modeling and the control methods, the integration work is carried out. The results are presented in Figure 4 for ESS charging mode and Figure 5 for ESS discharging mode. From the simulation results, the performance of the voltage regulation and the ESS are observed. As it is expected, the response of the supercapacitor is much faster than that of the battery, and it leads to the oscillations in the power load profile in the grid. In addition, the voltages are controlled at their required level with the controllers.

TABLE III
Power System and Electric Circuit Parameters

Parameter	Value
V_{AC}	690 V
V_{DC}	1000 V
V_{sc}	300 V / 200 V (max/min)
V_{batt}	850 V (nominal)
V_{cpl}	1000 V
V_{cil}	230 V
P_{cpl}	7000 kW
P_{cil}	1730 kW
$L_{g,a}$	27.9 mH
$r_{g,a}$	4.5 Ω
$L_{r,a}$	27.9 mH
$r_{r,a}$	4.5 Ω
C_{LCL}	120 μF
$f_{sw,rec}$	15 kHz
f_{grid}	50 Hz

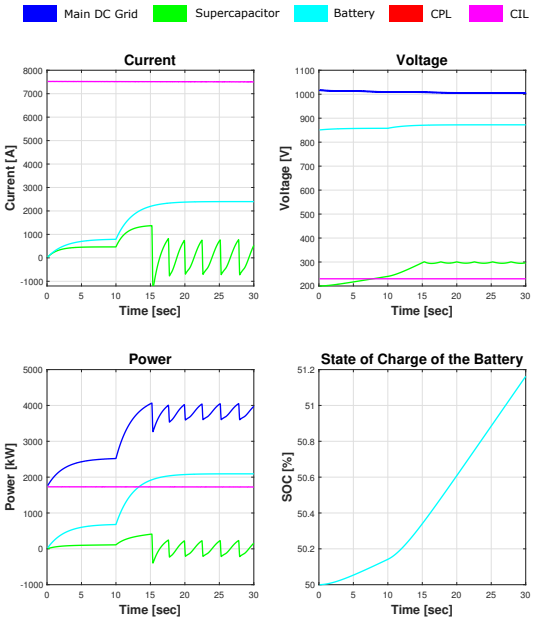

Fig. 4. Simulation Result of Onboard DC Power System (ESS Charging)

V. Stability Analysis

The constant power load (CPL) in Figure 1 represents propulsion motor drives which are regulated tightly with controllers and other minor loads are summed as a resistance

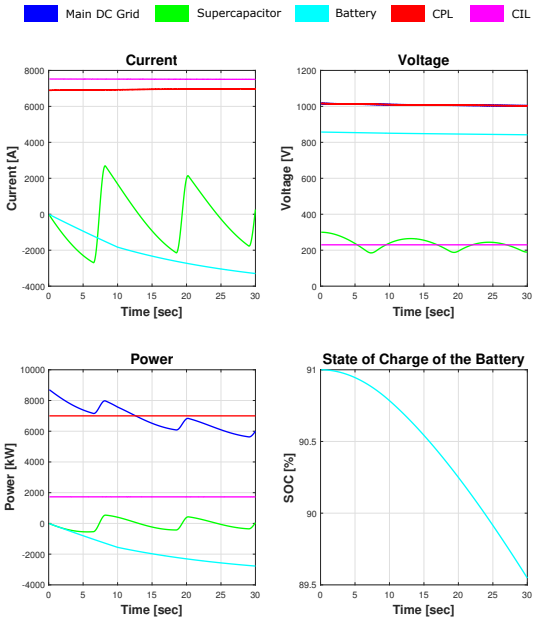

Fig. 5. Simulation Result of Onboard DC Power System (ESS Disharging)

(constant impedance load). Since these loads can affect the stability of the power system, the stability analysis should be carried out for the design of the system. The load equations in Section II are rewritten with states x_1 - x_6, and the system has nonlinearity due to the CPL in (19) and the duty cycle for DC/DC converter control in (22). Therefore, the linearization of the load equation should be done as (27)-(29) with x_o and u_o as equilibrium points.

$$\delta\dot{\mathbf{x}} = \mathbf{A}(\mathbf{x_o}, \mathbf{u_o})\delta\mathbf{x} + \mathbf{B}(\mathbf{x_o}, \mathbf{u_o})\delta\mathbf{u} \tag{27}$$

$$\delta\mathbf{x} = [\delta i_{cpl,1}, \delta V_{fl,1}, \delta i_{cil,1}, \delta V_{fl,2}, \delta i_{cil,2}, \delta V_{ld,2}]^T \tag{28}$$

$$\delta\mathbf{u} = [\delta V_{dc}, \delta P_{CPL}, \delta d]^T \tag{29}$$

Then, the linearized system in state-space form can be obtained with matrices $A(x_o, u_o)$ and $B(x_o, u_o)$ as:

$$\mathbf{A}(\mathbf{x_o}, \mathbf{u_o}) = \begin{bmatrix} -\frac{r_{fl,1}}{L_{fl,1}} & -\frac{1}{L_{fl,1}} & 0 & 0 & 0 & 0 \\ \frac{1}{C_{fl,1}} & \frac{P_{CPL,o}}{C_{fl,1}x_{2,o}^2} & 0 & 0 & 0 & 0 \\ 0 & 0 & -\frac{r_{fl,2}}{L_{fl,2}} & -\frac{1}{L_{fl,2}} & 0 & 0 \\ 0 & 0 & \frac{1}{C_{fl,2}} & 0 & -\frac{1}{C_{fl,2}} & 0 \\ 0 & 0 & 0 & \frac{1}{L_{ld,2}}d_o & 0 & -\frac{1}{L_{ld,2}} \\ 0 & 0 & 0 & 0 & \frac{1}{C_{ld,2}} & -\frac{1}{C_{ld,2}r_{cil}} \end{bmatrix} \tag{30}$$

$$\mathbf{B}(\mathbf{x_o}, \mathbf{u_o}) = \begin{bmatrix} \frac{1}{L_{fl,1}} & 0 & 0 \\ 0 & -\frac{P_{CPL,o}}{C_{fl,1}x_{2,o}} & 0 \\ \frac{1}{L_{fl,2}} & 0 & 0 \\ 0 & 0 & 0 \\ 0 & 0 & \frac{1}{L_{ld,2}}x_{4,o} \\ 0 & 0 & 0 \end{bmatrix} \tag{31}$$

From the linearized system, the eigenvalues are calculated with a different value of DC voltage and CPL. Then, the stable and unstable region is determined by using the Hurwitz stability criterion as shown in Figure 6.

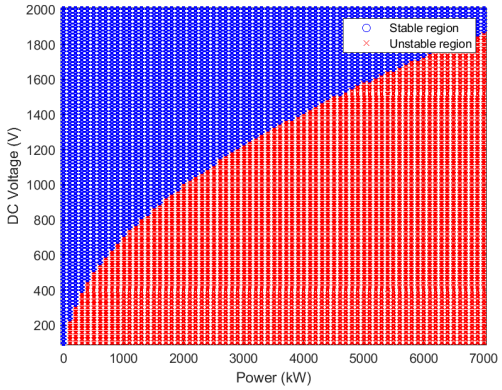

Fig. 6. Stable and unstable region with varying CPL and DC voltage

The results show that the current DC voltage set limits the single CPL up to around 2,000 kW. Otherwise, the DC voltage level must be elevated. Current 7,000 kW as a single CPL causes instability in the power system, so the CPL is divided into four parts with each LC filter. Figure 7 shows the eigenvalues of the modified system. All the negative eigenvalues are observed for the system to be Hurwitz stable.

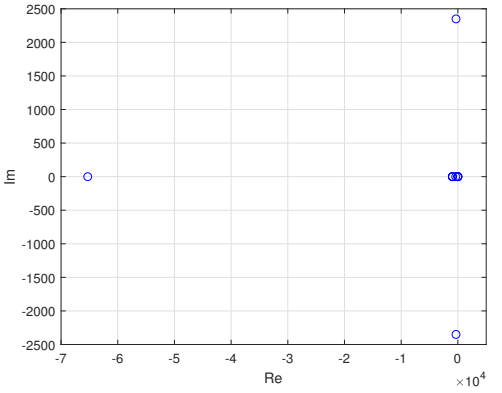

Fig. 7. Eigenvalue plot for the reduced CPL

VI. Conclusion

In this paper, a dynamic model has been developed and applied for the stability analysis and advanced control method of onboard DC power system. Although some simplifications have been made to improve the simulation time, the simulations show the effectiveness of the proposed model. In addition, the stability analysis explains the causes of the instability in the power system so that the relevant measures can be taken. As a further study, detailed modeling of the power converters can be done to observe the instability problems from their rapid switching.

References

[1] A. Alacano, J. J. Valera, G. Abad, and P. Izurza "Power-Electronic-Based DC Distribution Systems for Electrically Propelled Vessels: A Multivariable Modeling Approach for Design and Analysis", *IEEE Journal of Emerging and Selected Topics in Power Electronics*, vol.5, no.4, pp.1604-1620, 2017.

[2] M. K. Zadeh, R. Gavagsaz-Ghoachani, S. Pierfederici, B. N. Mobarakeh and M. Molinas "Stability analysis of hybrid AC/DC power systems for More Electric Aircraft", *IEEE Applied Power Electronics Conference and Exposition (APEC'16)*, 2016.

[3] M. Armstrong, C. Ross, D. Phillips, and M. Blackwelder,"Stability, Transient Response, Control, and Safety of a High-Power Electric Grid for Turboelectric Propulsion of Aircraft", *NASA/CR Report No. 2013-217865*, 2013.

[4] M. K. Zadeh, B. Zahedi, M. Molinas, and L. E. Norum "Centralized stabilizer for marine DC microgrid", *39th Annual Conference of the IEEE Industrial Electronics Society (IECON 2013)*, Vienna, 2013.

[5] M. K. Zadeh, R. Gavagsaz-Ghoachani, J-P. Martin, S. Pierfederici, B. N. Mobarakeh and M. Molinas "Discrete-Time Tool for Stability Analysis of DC Power Electronics-Based Cascaded Systems", *IEEE Transactions on Power Electronics*, vol.32, no.1, pp.652-667, 2017.

[6] M. K. Zadeh, R. Gavagsaz-Ghoachani, J-P. Martin, S. Pierfederici, B. N. Mobarakeh and M. Molinas "Discrete-Time Modeling, Stability Analysis, and Active Stabilization of DC Distribution Systems With Multiple Constant Power Loads,", *IEEE Transactions on Industry Applications*, vol.52, no.6, pp.4888-4898, 2016.

[7] M. K. Zadeh, S. Pierfederici, B. N. Mobarakeh and M. Molinas "Stability Analysis and Dynamic Performance Evaluation of A Power Electronics-Based DC Distribution System With Active Stabilizer", *IEEE Journal of Emerging and Selected Topics in Power Electronics*, vol.4, no.1, pp.93-102, 2016.

[8] A. Emadi, "Modeling and analysis of multi-converter DC power electronic systems using the generalized state-space averaging method", *IEEE Transactions on Industrial Electronics*, vol.51, no.3, pp.661-668, 2004.

[9] D. Maksimović, A. M. Stanković, V. J. Thottuvelil and G. C. Verghese, "Modeling and Simulation of Power Electronic Converters", *Proceedings of the IEEE*, vol.89, no.6, pp.898-912, 2001.

[10] B. Zahedi, and L. E. Norum, "Modeling and simulation of all electric ships with low-voltage dc hybrid power systems", *IEEE Transactions on Power Electronics*, vol.28, no.10, pp.4525-4537, 2013.

[11] S. R. Sanders, J. M. Noworolski, X. Z. Liu and G. C. Verghese, "Generalized averaging method for power conversion circuits", *IEEE Transactions on Power Electronics*, vol.6, no.2, pp.251-259, 1991.

[12] C. M. Shepherd, "Design of primary and secondary cells - part 2. An equation describing battery discharge", *Journal of Electrochemical Society*, vol.112, pp.657-664, 1965.

[13] O. Tremblay, and L. A. Dessaint, "Experimental validation of a battery dynamic model for EV applications", *World Electric Vehicle Journal*, vol.3, pp.289-298, 2009.

[14] K-N. Areerak, S. V. Bozhko, G. M. Asher and D.W. P. Thomas, "DQ-Transformation Approach for Modelling and Stability Analysis of AC-DC Power System with Controlled PWM Rectifier and Constant Power Loads", *13th International Power Electronics and Motion Control Conference (EPE-PEMC 2008)*, Poznan, Poland, Sept. 2008, pp.2049-2054.

[15] M. K. Zadeh, L. M. Saublet, R. Gavagsaz-Ghoachani, S. Pierfederici, B. N. Mobarakeh and M. Molinas "Energy management and stabilization of a hybrid DC microgrid for transportation applications", *IEEE Transactions on Power Electronics*, vol.32, no.1, pp.652-667, 2017.

[16] M. K. Zadeh, L. M. Saublet, R. Gavagsaz-Ghoachani, J-P. Martin, S. Pierfederici, B. N. Mobarakeh and M. Molinas "A new discrete-time modelling of PWM converters for stability analysis of DC microgrid", *ELECTRIMACS 2014, International Conference on Modeling and Simulation of Electric Machines, Converters and Systems*, Valencia, Spain, May 2014.